



A Simple Equation for Predicting Superconformal Electrodeposition in Submicrometer Trenches

D. Josell,^z D. Wheeler, W. H. Huber, J. E. Bonevich, and T. P. Moffat*

National Institute of Standards and Technology, Metallurgy Division, Gaithersburg, Maryland 20899, USA

We present a single variable first-order differential equation for predicting the occurrence of superconformal electrodeposition. The equation presumes that the dependence of deposition rate on surface coverage of the accelerator is known (*e.g.*, derived from voltammetry experiments) on planar electrodes. A simplified growth geometry, based on the recently proposed mechanism of curvature enhanced accelerator coverage, is used to permit simplification of the trench-filling problem. The resulting solution is shown to reduce computational time from hours to seconds, while yielding reasonably accurate predictions of the parameter values required for trench filling.

© 2001 The Electrochemical Society. [DOI: 10.1149/1.1414287] All rights reserved.

Manuscript received July 11, 2001. Available electronically November 2, 2001.

State of the art manufacturing of semiconductor devices involves electrodeposition of copper for device wiring. Successful implementation in Damascene processing has resulted in enhanced performance and significant cost reduction.¹ Interestingly, implementation of copper electroplating has proceeded in the absence of a robust physical description of the feature filling process. In addition, operational parameters remain a highly sensitive proprietary issue. This combination of factors has hindered process optimization and limited scientific assessment of future prospects for this technology. Early modeling studies focused on leveling theory where the location-dependent growth rate derived from diffusion limited accumulation of an inhibiting species.² However, this formulation was unable to predict several key experimental observations.³⁻⁶ Recently a model electrolyte for the study of superconformal electrodeposition was identified⁶ along with a curvature enhanced accelerator coverage model that provides a quantitative description of superconformal deposition.^{7,8} The fundamental premise of the model is that the dilute accelerating thiol or disulfide derived from a 3-mercaptopropanosulfonate additive (MPSA) adsorbs strongly on the surface, thereby displacing the inhibiting polymeric species derived from polyethylene glycol and chloride (PEG-Cl) additives. In the model all adsorbed species remain on or float at the surface during deposition. In the case of nonplanar substrates, compression of adsorbed accelerator with reduction of surface area during growth, such as occurs at points of positive curvature (*e.g.*, the bottoms of small trenches), results in increased local velocity. A front tracking code was used to demonstrate that such a mechanism, using an experimentally derived relationship for the dependence of deposition rate on adsorbed accelerator, could generate superconformal electrodeposition. The model and associated front-tracking code assumed the cupric ion and additive concentrations to be independent of position in the electrolyte near the surface.⁷ Model predictions were shown to agree with experimental results for filling of trenches between 350 and 100 nm wide and 500 nm deep over a wide range of processing conditions. A second model that includes an explicit solution of the diffusion equations that govern copper and accelerator arrival through the electrolyte to the surface has also been published;⁸ a code using the level-set method rather than front-tracking was used for the simulations.

An alternative model based on accumulation of accelerator at the bottom of features was recently published.⁹ The simulation parameters were tuned in order to obtain agreement with fill studies for one particular electrolyte composition, *e.g.*, an equilibrium surface coverage of the accelerator of 0.05 was used. This value is well below the near-unity equilibrium coverage used in this work and Ref. 6, 7, and 8.

Based on the concept of "curvature enhanced accelerator cover-

age" from Ref. 7 and 8, a simple geometrical model is presented that captures the fundamentals of the near-optimized filling mechanism while reducing the problem to a first-order differential equation that can be solved in less than a second. In contrast, the front-tracking code that neglects diffusion⁷ required approximately 30 min to simulate the filling of one trench, and the level-set code that includes diffusion required several hours on the same computer (with a 1 GHz clocked processor) for each simulation. This new model is referred to as the "simple" model. Its simplicity permits a study of the potential and concentration dependence of trench filling over a range of aspect ratios to be performed in less time than is required to generate a single solution for one concentration and aspect ratio using either the front-tracking or level-set codes.

For model validation, predictions of the simple model are compared with results from the level-set code, which, to reiterate, solves for the space and time dependent cupric ion and accelerator concentrations in the electrolyte and uses the actual interface shape. The predictions of the simple model are also compared to experimental results. Predictions of the simple model are seen to be in good agreement with the level-set code predictions as well as experimental results for the range of parameter space over which superfilling occurs. There is only a modest loss of predictive ability at the boundary between conditions which yield superfill (fill) *vs.* those that lead to void formation (fail).

The Simple Model

Determination of equations of evolution.—The approximations in the simple model, the validity of which are discussed later, are as follows. The time-dependent interface shape is approximated for all times by vertical and horizontal line segments for the moving sides and bottom, respectively (Fig. 1). Filling of a trench of width w and height h is monitored by tracking the location at which the bottom and side surfaces meet as a function of time, *i.e.*, $z(t) = [x(t), y(t)]$, shown schematically in Fig. 1. The simple model and numerical level set code use the same experimentally derived relationship for velocity v and the surface coverage θ of accelerator ($v = i(\theta)\Omega/2F$ with $i(\theta)$ the current density, Ω , the atomic volume of copper, and F , Faraday's constant). The local growth rate v has been shown to increase monotonically with the surface coverage of accelerator θ and overpotential η ^{6,8} and scales linearly with the cupric ion concentration C at the interface, having the form

$$v(\theta, \eta, C) = \frac{C}{C_{\text{Cu}}} v_0(\theta) \exp\left(-\frac{\alpha(\theta)F}{RT} \eta\right) \quad [1]$$

The accumulation of accelerator from the electrolyte to the surface is approximated to have no explicit spatial variation within the feature. It is expressed in terms of the concentration of the additive in

* Electrochemical Society Active Member.

^z E-mail: josell@nist.gov

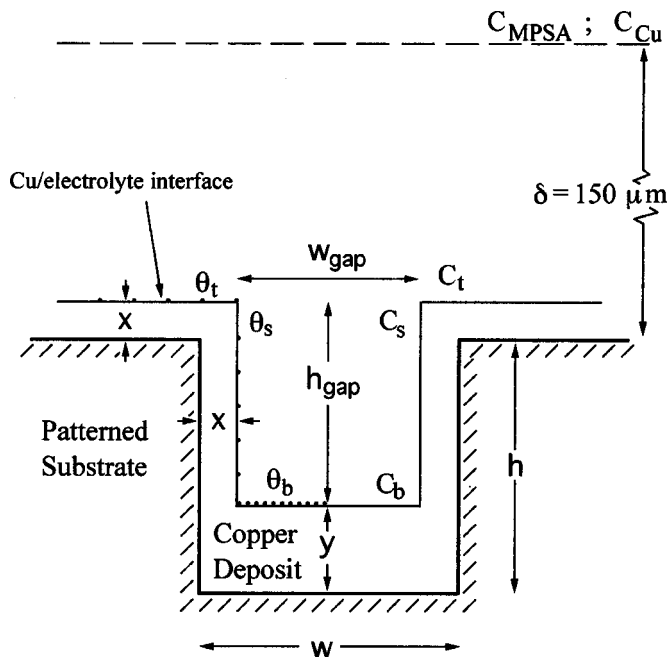


Figure 1. A schematic of the approximate geometry used for the simple model. Included are definitions of the dimensions, growth rates, concentrations within the electrolyte, and surface coverage θ of accelerator on different surfaces (equal to $1 - \theta$ coverages of inhibitor). Due to assumptions within the model, the growth of the sidewalls equals that on the top surface. Also indicated is the boundary layer over which diffusion of cupric ion and accelerator occurs.

the bulk electrolyte C_{MPSA} , the diffusion coefficient D_{MPSA} , the number of available sites $\Gamma(1 - \theta)$ and a potential dependent rate constant $k(\eta)$ by Ref. 8

$$\frac{d\theta_t}{dt} = \frac{C_{MPSA}k(1 - \theta_t)}{1 + \delta\Gamma k(1 - \theta_t)/D_{MPSA}} \quad [2]$$

where $k = 1.8 \times 10^5 - 2.7 \times 10^7 \eta^3$ [$\text{cm}^3/\text{mol s}$], $D_{MPSA} = 1 \times 10^{-5} \text{ cm}^2/\text{s}$, the thickness of the boundary layer is $\delta = 150 \mu\text{m}$, the areal density of absorption sites is $\Gamma = 9.7 \times 10^{-10} \text{ mol}/\text{cm}^2$, and the accumulation is zero at zero time $\theta_t(0) = 0$. Equation 2 captures the gradient of concentration across the boundary layer as well as the equality of the flux diffusing across the boundary layer and attaching to the interface. With the rate of accumulation defined by Eq. 2, the accelerator adsorbed on the interface saturates at unity coverage (one monolayer). As is done in the level-set calculations,⁸ a value of $\theta = 1$ is used when areal shrinkage makes θ rise above unity (excess is thus implicitly destroyed or incorporated into the deposited copper).

For potentiostatic deposition (fixed η), the horizontal displacements of the sidewalls, x , is expressed in terms of their accelerator coverage θ_s and the local cupric ion concentration C_s

$$x(t) = \int_0^t v[\theta_s(t), C_s(t)] dt \equiv \int_0^t v_s(t) dt \quad [3]$$

and, likewise, the vertical displacement of the bottom surface can be expressed in terms of its accelerator coverage θ_b and the local cupric ion concentration C_b

$$y(t) = \int_0^t v[\theta_b(t), C_b(t)] dt \equiv \int_0^t v_b(t) dt \quad [4]$$

Next it is postulated that the evolution of accelerator coverage on the sidewalls of the trench, $\theta_s(t)$, is identical to that occurring on the free surface (as given in Eq. 2), *i.e.*, no significant depletion occurs down the trench

$$\frac{d\theta_s}{dt} = \frac{C_{MPSA}k(1 - \theta_s)}{1 + \delta\Gamma k(1 - \theta_s)/D_{MPSA}} \quad [5]$$

Equation 5 can be evaluated numerically to obtain $\theta_s(t)$ given that $\theta_s(0) = 0$. Note that $\theta_s(t) = \theta_t(t)$. The coverage on the bottom surface, $\theta_b(t)$, is postulated to follow

$$\frac{d\theta_b}{dt} = \frac{C_{MPSA}k(1 - \theta_b)}{1 + \delta\Gamma k(1 - \theta_b)/D_{MPSA}} + \frac{2\theta_s v_b}{w - 2x} + \frac{2\theta_b v_s}{w - 2x} \quad [6]$$

where, again, $\theta_b(0) = 0$. As with Eq. 5 for the sidewalls, the first term in Eq. 6 represents the accumulation from the electrolyte. The last two terms represent accrual of the accelerator that was on the sidewall region eliminated by the upward motion of the bottom and the concentrating effect of the shrinking bottom, respectively; $w - 2x$ is the time-dependent width of the bottom (Fig. 1). Equation 6 is a nonlinear first-order differential equation in θ_b . It can be used, with the experimentally derived parameters and Eq. 1 to solve for $\theta_b(t)$.

From Eq. 3, the time t^* at which the sidewalls would reach the midline of the trench width w , is defined by

$$x(t^*) \equiv \frac{w}{2} \quad [7]$$

The criterion for trench filling is that the bottom surface escapes from the trench mouth before the sides close in, leaving a seam (or void). This can be written as

$$y(t^*) \geq h \quad [8]$$

with t^* determined from Eq. 7 and $y(t)$ from Eq. 4. The equality holds at the transition between conditions that lead to fill *vs.* those that lead to formation of a seam (or void). The conditions for fill are now expressed in terms of the functions $v(\theta, C, \eta)$ and the geometrical consequences of growth in the trench as per Eq. 6. The evolution of the quantities $\theta_b(t)$, $\theta_s(t)$, $v_b(t)$, and $v_s(t)$ [thus $y(t)$ and $x(t)$] can be numerically evaluated using Eq. 1-6 once the cupric ion concentrations $C_s(t)$ and $C_b(t)$ are known (see Eq. 3 and 4). This model can be easily extended to via geometry by considering the additional compression term associated with sidewall motion.

Accounting for the effects of cupric ion depletion.—The deposition rate $v(\theta = 1)/v(\theta = 0)$ goes from 30 to 300 for η from -0.1 to -0.3 V (absent cupric ion limitations). Thus, if the accelerator coverage on the bottom surface saturates while the sidewalls still have low coverage, then the criterion in Eq. 8 will predict that the bottom can escape even if the unfilled region has an aspect ratio much greater than 10. In such a case, diffusional limitations will certainly lead to the breakdown of several of the assumptions made to derive the above fill criterion. The impact of cupric ion Cu^{2+} depletion will therefore be determined.

Mass balance of the copper ion flux at the top of the gap (see Fig. 1) with the consumption of copper associated with motion of the sidewalls and bottom gives

$$w_{\text{gap}} \Omega_{\text{Cu}} D_{\text{Cu}} \nabla C|_{\text{top}} = 2h_{\text{gap}} v_s + w_{\text{gap}} v_b \quad [9]$$

with cupric ion diffusion coefficient $D_{\text{Cu}} = 5 \times 10^{-6} \text{ cm}^2/\text{s}$ and $\Omega_{\text{Cu}} = 7.1 \text{ cm}^3/\text{mol}$. In keeping with the approximate nature of this solution, ∇C is approximated as constant down the trench, with all cupric ion consumption by the sidewalls approximated as occurring at the bottom of the trench. By the point that depletion becomes

substantial and this approximation is no longer valid, the assumption of uniform sidewall velocity is already invalid (see Eq. 1). For the conditions of interest in this study, this occurs only when the sidewalls have approached close enough that failure to fill is imminent. The time-dependent concentrations of cupric ion at the bottom (C_b) and top (C_t) of the trench are related by

$$C_b(t) \equiv \beta C_t(t) \quad [10]$$

Thus defined, $\beta(t) \leq 1$ during deposition, and $\nabla C = C_t(1 - \beta)/h_{\text{gap}}$. Equation 9 thus becomes

$$w_{\text{gap}} \Omega_{\text{Cu}} D_{\text{Cu}} \frac{C_t(1 - \beta)}{h_{\text{gap}}} = 2h_{\text{gap}} v_s + w_{\text{gap}} v_b \quad [11]$$

For an isolated trench, the exact solution requires consideration of the hemicylindrical diffusional field in the electrolyte. The exact solution for the case of a periodic array of trenches, while approaching one-dimensional diffusion far from the surface (compared to feature spacing), will be affected by the additional consumption associated with growth of the sidewalls.⁸ This effect is largest for the filling of high aspect ratio features that are closely spaced with deposition under conditions of mixed control [when $\Gamma \delta k(1 - \theta)/D_{\text{MPSA}} \approx 1$, as per Eq. 2]. For conditions studied here, the diffusion field is treated as that above a planar surface.⁸ In this case, the concentration of cupric ion at the top of the trench C_t can be written as a function of the bulk concentration C_{Cu} in the electrolyte. This is done by invoking mass balance of the cupric ion flux across the boundary layer and the copper incorporation into the top surface, moving at velocity $v_t(t)$, to obtain⁸

$$\Omega_{\text{Cu}} D_{\text{Cu}} \frac{C_{\text{Cu}} - C_t}{\delta} = v_t \quad [12]$$

The cupric ion concentration for the sidewalls (C_s) is approximated as equal to that at the top of the trench (C_t), which will yield an upper bound of sidewall velocity. Because the accumulation of accelerator on the sidewalls is modeled as independent of position, thus also equivalent to that on the top surface, the growth rate on the sidewalls (v_s) equals that on the top surface (v_t). This approximation models void formation through more rapid sidewall growth near the top of the trench where there is less cupric ion depletion. Replacing C_t and v_t by C_s and v_s , respectively, Eq. 12 can be rewritten as

$$C_s(t) = C_{\text{Cu}} - \frac{\delta v_s}{\Omega_{\text{Cu}} D_{\text{Cu}}} \quad [13]$$

and Eq. 11 and 12 can be solved for β to obtain

$$\beta = 1 - \frac{h_{\text{gap}}}{w_{\text{gap}}} (2h_{\text{gap}} v_s + w_{\text{gap}} v_b) / (C_{\text{Cu}} \Omega_{\text{Cu}} D_{\text{Cu}} - \delta v_s) \quad [14]$$

The dimensions of the unfilled gap region can be replaced using $h_{\text{gap}} = h + x - y$ and $w_{\text{gap}} = w - 2x$ (see Fig. 1) to obtain

$$\beta(t) = 1 - \frac{(h + x - y) [2(h + x - y)v_s + (w - 2x)v_b]}{(w - 2x) (C_{\text{Cu}} \Omega_{\text{Cu}} D_{\text{Cu}} - \delta v_s)} \quad [15]$$

Finally, using Eq. 13 and 15

$$C_b(t) = \left(1 - \frac{(h + x - y) [2(h + x - y)v_s + (w - 2x)v_b]}{(w - 2x) (C_{\text{Cu}} \Omega_{\text{Cu}} D_{\text{Cu}} - \delta v_s)} \right) \times \left(C_{\text{Cu}} - \frac{\delta v_s}{\Omega_{\text{Cu}} D_{\text{Cu}}} \right) \quad [16]$$

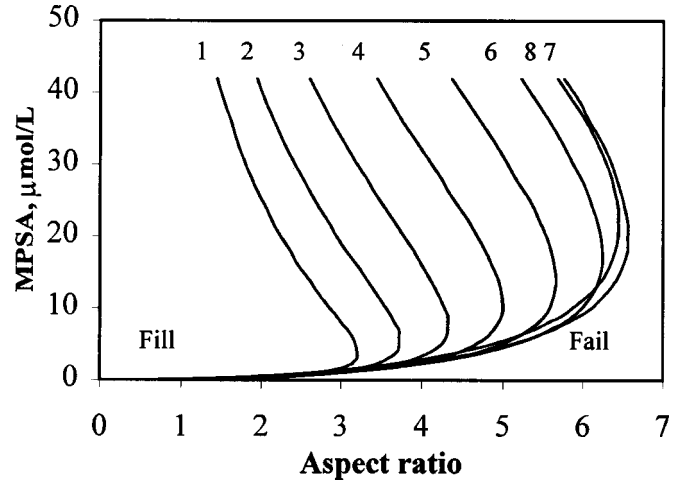


Figure 2. Fill/fail boundaries predicted by the simple model as a function of the concentration of accelerator in the electrolyte are shown for representative overpotentials. Curves are enumerated according to overpotential in -0.02 V increments, *i.e.*, (1) -0.14 , (2) -0.16 , (3) -0.18 , (4) -0.20 , (5) -0.22 , (6) -0.24 , (7) -0.26 , and (8) -0.28 V. Fill occurs at lower aspect ratios (left of appropriate fill/fail boundary), and fail occurs at higher aspect ratios (right of appropriate boundary).

The time-dependent decrease of C_s below the bulk value C_{Cu} (Eq. 13) comes from the drop across the boundary layer required to supply the increasing cupric ion consumption associated with the increasing surface coverage of accelerator. The concentration at the bottom of the trench (Eq. 16) reflects this effect as well as additional depletion down the trench itself due to cupric consumption by both the sidewalls and the bottom.

The expressions for the cupric concentrations $C_s(v_s)$ and C_b (v_b, v_s) in Eq. 13 and 16, respectively, with the empirical formulas $v_s(C_s)$ and $v_b(C_b)$ defined in Eq. 1, 3, and 4, provide four nonlinear equations that are solved for the unknown $C_b, C_s, v_b,$ and v_s . With Eq. 5 and 6 defining the impact of the growth rates v_s and v_b on the evolution of the surface coverages θ_s and θ_b , the equations describing trench filling in the simple model are now fully determined.

Predictions of the Model

Comparison to the level-set code predictions.—Figure 2 shows model predictions, specifically whether fill or fail is to be expected, for the experimentally derived velocity function⁸

$$v(\theta, \eta, C) = \frac{\Omega_{\text{Cu}} C}{2F C_{\text{Cu}}} (0.069 + 0.64\theta) \times \exp\left(-\frac{(0.447 + 0.299\theta)F}{RT} \eta\right) \quad [17]$$

with $C_o = 2.5 \times 10^{-4}$ mol/cm³, $F = 96,485$ C/mol, $R = 8.314$ J/mol K, and $T = 293$ K, and other parameters as given earlier. The trench depth h used for the fill criterion in Eq. 8 is 0.5 μm ; this value is used for all modeling. The curves delineate the border between fill vs. fail conditions for a series of deposition voltages. Perhaps the most important feature of Fig. 2 is the existence of an optimal range of accelerator concentrations C_{MPSA} . This can be understood via the model. Too low a value leads to inadequate coverage θ_b and inadequate upward acceleration of the bottom surface, even with geometrical compression. Too high a value leads to near-unity coverage θ_s (as well as θ_b) and thus equal, albeit high, velocities for all surfaces (conformal growth). The generally improved filling with overpotential η going from -0.14 to -0.26 V is associated with the increase of the ratio $v(\theta = 1)/v(\theta = 0)$ with η that was noted earlier. The maximization and subsequent decrease (not

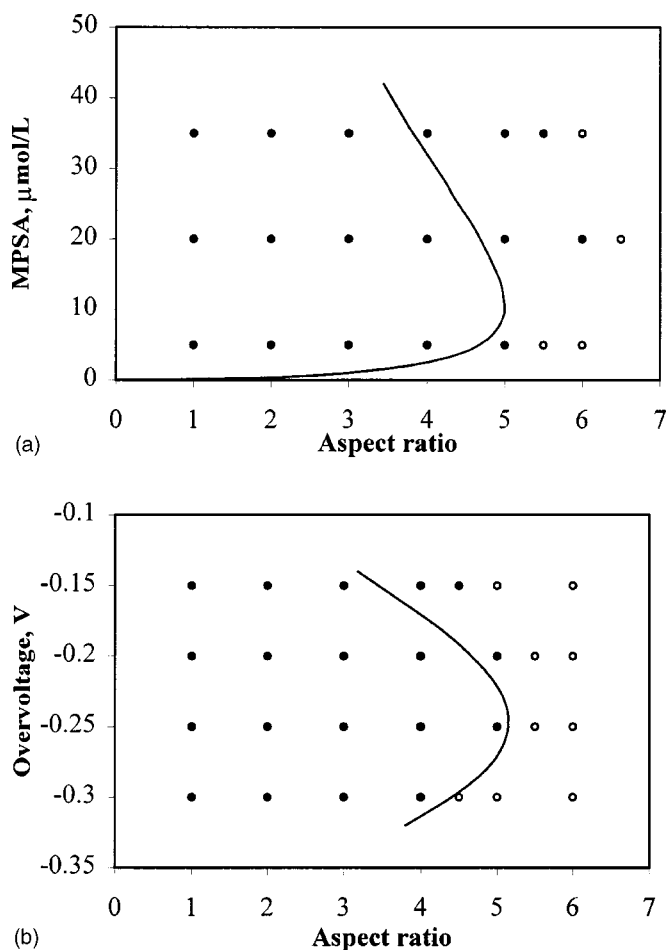


Figure 3. (a, top) Fill/fail boundaries predicted by the simple model are compared to level-set code predictions at overpotentials of -0.2 V as a function of the concentration of accelerator in the electrolyte. Filled circles indicate aspect ratios that filled according to the level-set code, while open circles indicate those that developed voids (superfill). (b, bottom) Fill/fail boundaries predicted by the simple model are compared to level-set predictions for an accelerator concentration of $5 \mu\text{mol/L}$ as a function of the overpotential η during deposition.

shown) of predicted fill conditions with potential are caused by inadequate C_b for the higher deposition rates and decreasing fill times associated with these higher overpotentials; cross-over of the boundaries at low accelerator concentration ($C_{MPSA} < 5 \mu\text{mol/L}$), not resolvable in Fig. 2, is also caused by this. Clearly, the ability of an electrolyte to fill trenches of a given aspect ratio depends strongly on the bulk concentration of the additive in the electrolyte (C_{MPSA}) and the overpotential. It is worth noting that, under optimal conditions, superfilling is predicted to occur in features with aspect ratios exceeding 6. Use of higher cupric ion concentrations will push this value higher, though the exact value is uncertain as kinetics have not been fully determined for such electrolyte concentrations.

Figure 3 compares predictions of the simple model with results obtained using the level-set code. Figure 3a shows the predicted boundary between fill/fail conditions for overpotential $\eta = -0.2$ V; the predictions of the level-set code are shown by open (solid) circles for void formation (superfill). Agreement of the border predicted by the simple model of this paper and the border between fill/fail of the level-set code data points for C_{MPSA} up to $\approx 5 \mu\text{mol/L}$ is good. The number of the level-set data points is limited by the computational demands of the code, noted earlier. Agreement in trend though not absolute value is noted between the simple model and level-set code predictions at higher C_{MPSA} , with the

simple model underestimating the maximum filling aspect ratio by ≈ 1 for C_{MPSA} greater than $\approx 20 \mu\text{mol/L}$. Figure 3b shows the impact of overpotential on the predicted boundary between fill/fail conditions for $C_{MPSA} = 5 \mu\text{mol/L}$. Again, the predictions of the level-set code are shown by open (solid) circles for void formation (superfill). The simple model captures the maximum filling aspect ratio of approximately 5, the predicted voltage dependence shifted by ≈ 50 mV from the level-set solution.

Growth contours as predicted by the simple model and the level-set code are compared in Fig. 4a (left and right, respectively).³ Growth in the simple model is shown until the trench is filled. Modeling beyond when the bottom surface extends above the top surface (at height $h + x$), forming the bump visible over the filled trench from the level-set code simulation, requires extension of the simple model. It is evident that the use of vertical sidewalls and horizontal bottom successfully captures the essence of the growth profile up to the point of surface inversion. Figure 4b shows the corresponding histories of y and x , the copper deposition thickness from the trench bottom and sides, in the simple model. Feature filling is indicated by the fact that y reaches the trench height ($0.5 \mu\text{m}$) before x reaches the trench half-width. Figure 4c shows the corresponding histories of θ_b and θ_s , the accelerator coverages on the bottom interface and side interfaces. Figure 4d shows the corresponding histories of C_b and C_s , the cupric ion concentrations at the bottom and sides of the unfilled region. It is evident from Fig. 4b that nearly 80% of the y displacement of the bottom surface occurs in the last 3 s, after the accelerator coverage on the bottom surface has saturated (Fig. 4c) giving maximum growth rate. The general decrease in cupric ion concentrations (Fig. 4d) is caused by the increasing deposition rates on all surfaces (top, sidewalls, and bottom) associated with the accumulation of the accelerator (Fig. 4c). The rapid decrease of C_b at ~ 25 s in particular (Fig. 4d) is caused by the increasing gradient of concentration required to supply the accelerating deposition rate on the bottom surface. The sudden change of slope at ~ 26 s (Fig. 4d) is caused by attainment of $\theta_b = 1$ (Fig. 4c) which halts further increase of the velocity of the bottom surface. With the velocity of the bottom surface, and thus cupric consumption, now nearly maximized, the gap height over which the gradient exists rapidly decreases and the cupric concentration C_b approaches $C_t (= C_s)$. This increase of C_b does lead to an increase in the velocity of the bottom surface (Eq. 1) and thus the slope of $y(t)$ for $t > 26$ s in Fig. 4b. However, this $\sim 30\%$ increase in velocity due to the reversal of the cupric depletion is insignificant in comparison to the 12,000% increase associated with saturation of the accelerator coverage in the first 25 s of deposition.

Analysis.—The relatively conservative predictions of the simple model as compared to the level-set calculations in Fig. 3a is likely due to the determination of sidewall velocity from cupric concentration at the top of the trench. As noted earlier, this simulates pinch-off at the top of the trench. Sidewall velocity obtained using the higher cupric concentration represents an upper bound and leads to more rapid closure (failure). This, in combination with the associated overestimate of cupric depletion down the trench, which leads to slower upward motion of the lower surface, is generally conservative. Though not done here, less conservative predictions can be obtained by using C_b equal to C_s (and C_t) as given by Eq. 13. This ignores cupric depletion down the trench, imposing only the concentration drop across the boundary layer.

It is unclear what role the instantaneous redistribution of accelerator on the bottom surface, implicit in Eq. 6, plays in the difference between the predictions of the level-set code and simple model. In the level-set simulations the accelerator coverage enriches earlier in the corners than in the middle of the bottom surface, which leads

³ The early level set code implemented for Ref. 8 did not accurately predict deposition at the upper corners. This inaccuracy did not impact the predictions for whether particular features filled, or failed to fill, in that work. It has been corrected here.

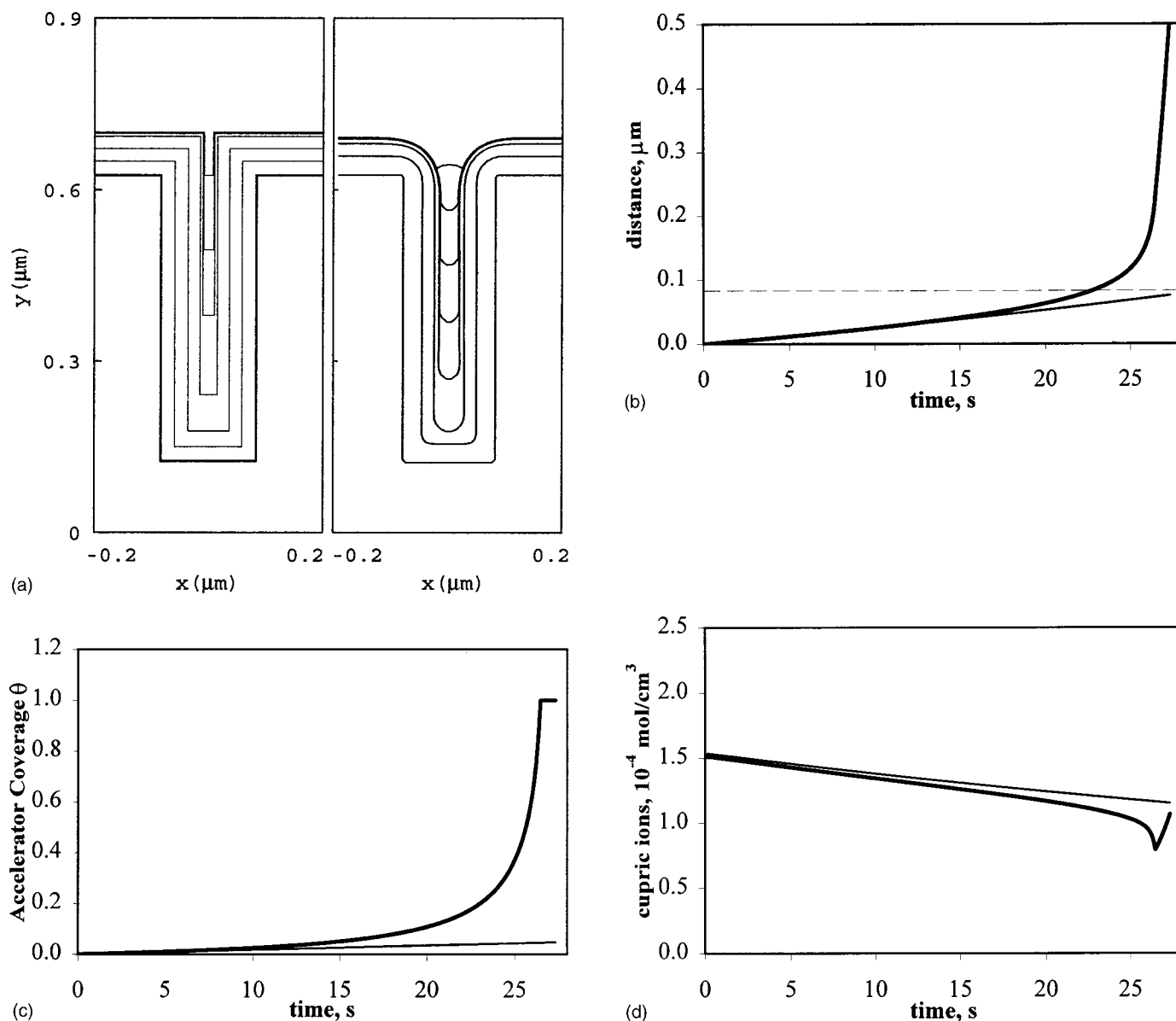


Figure 4. (a, top left) Filling contours predicted by the simple model (left) are compared to those obtained from the level-set code (right) for $C_{\text{MPSA}} = 5 \mu\text{mol/L}$ and $\eta = -0.282 \text{ V}$. The trenches are $0.5 \mu\text{m}$ deep with aspect ratio of 3 (height/width). Data associated with the simple model simulation: (b, top right) The corresponding histories of y and x , the copper deposition thickness from the trench bottom (bold line) and sides, respectively. The dashed line indicates the trench half-width. (c, bottom left) The corresponding histories of θ_b and θ_s , the accelerator coverages on the bottom interface (bold line) and side interfaces, respectively. (d, bottom right) The corresponding histories of C_b (bold line) and C_s , the cupric ion concentrations at the bottom and sidewalls, respectively, of the unfilled region.

to more rapid motion in the corners and curvature of the lower surface (Fig. 4a, right).

To study the impact of decreasing cupric ion and MPSA fluxes during the initial stages of deposition, a transient boundary layer thickness $\delta = \sqrt{\pi D_{\text{Cu}} t}$ was used for times t until δ reached the steady-state value of $150 \mu\text{m}$. Deposition rates of both Cu and MPSA-derivative increased significantly at early times (as per Eq. 1 and 12). However, this increased deposition occurred on both the bottom and side surfaces of the filling trench, causing shifts of the fill/fail boundary of less than 0.2 aspect ratio (not shown).

The impact of the simplifying assumptions made to derive the simple model has already been assessed through comparison of the simple model predictions with those of the level set calculations (Fig. 3). It is, nonetheless, worthwhile to examine the validity of the individual assumptions separately. First, as is assumed in the simple model, the level set calculations show that the bottom growth sur-

face is flat during the period of conformal growth (Fig. 4a, right). Once coverage of the accelerator saturates, though not flat, it maintains a near-constant shape. The sidewalls are flat at all times, as assumed in the simple model. The level set calculations show that there is less than a 10% drop of the accelerator and cupric ion concentrations going from the top of the trench to the bottom of the trench for most calculations;¹⁰ the position-independent accumulation of the accelerator from solution assumed in the simple model is therefore reasonable. Finally, the lower surface rapidly moves upward between the barely moving side walls in the level set calculations (Fig. 4a, right), sweeping up the adsorbed accelerator and compressing its own, consistent with the use of accumulation, transfer, and compressive terms for the coverage on the bottom surface versus simple accumulation for the sidewalls (Eq. 6 and 5, respectively).

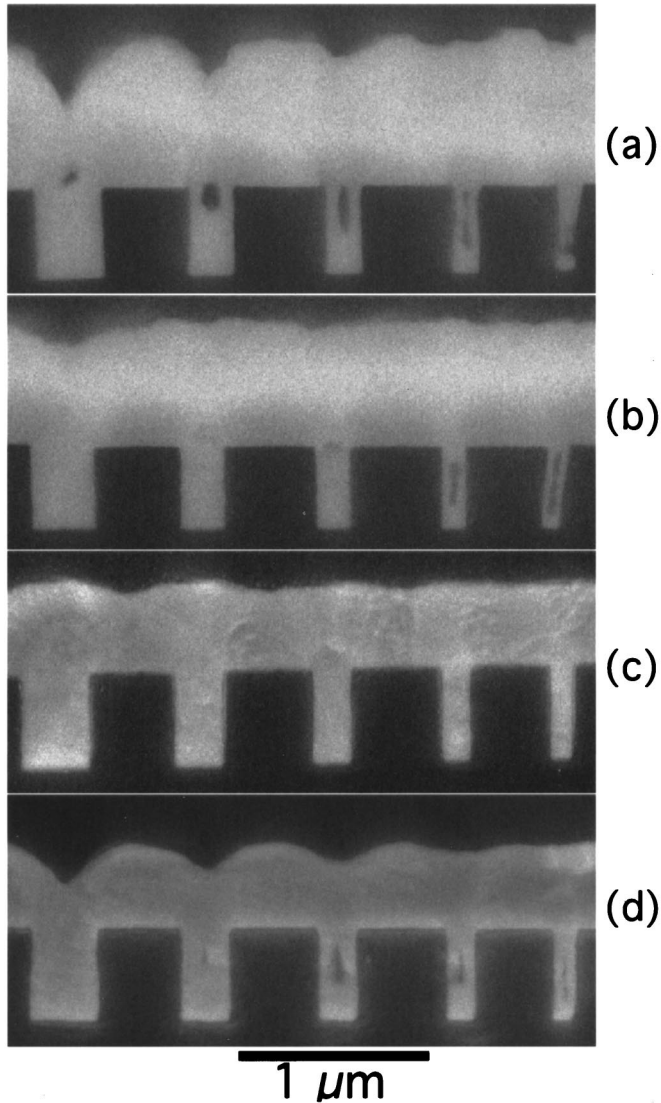


Figure 5. Images of trenches that have been filled and cross sectioned (obtained by scanning electron microscope). Lines are approximately $0.5 \mu\text{m}$ deep with linewidths varying between ≈ 350 and ≈ 100 nm. From top to bottom: (a) $\eta = -0.094$ V additive free; (b) $\eta = -0.301$ V and $C_{\text{MPSA}} = 0.5 \mu\text{mol/L}$; (c) $\eta = -0.282$ V and $C_{\text{MPSA}} = 5 \mu\text{mol/L}$; (d) $\eta = -0.150$ V and $C_{\text{MPSA}} = 40 \mu\text{mol/L}$.

Comparison to experimental data.—Model predictions were also compared to experimental results. The experimental technique has been detailed previously.⁶⁻⁸ Micrographs obtained by scanning electron microscope of typical experimental results are shown in Fig. 5 for conditions where some, none or all of the features filled. The transmission electron micrograph in Fig. 6 demonstrates that individual grains extend across filled features. Each specimen provides data points for multiple aspect ratios at a given overpotential and electrolyte chemistry. The height used for calculating the trench aspect ratio includes the 100 nm thick copper seed deposited by electron beam evaporation on the top surface of the trench prior to electrodeposition; 10 and 6 nm seeds on the trench bottom and sides, respectively, are ignored. Experimental data points, indicated by squares, are compared with predictions of the simple model in Fig 7. Filled (open) squares indicate that at least five of six examined features of that size were filled (voided). Crosses indicate a mixture of two to four filled/voided features, likely indicating discrete pores associated with roughness of the colliding sidewalls. Figure 7a compares experimental results for electrolytes with lower C_{MPSA} depos-

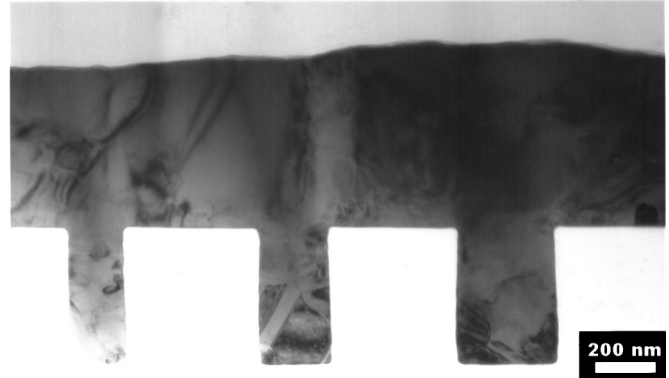


Figure 6. Image of trenches that have been filled and cross sectioned (obtained by transmission electron microscopy). Note that the filled trenches exhibit grains, with twins, extending across their full widths. Overpotential $\eta = -0.284$ V and $C_{\text{MPSA}} = 5 \mu\text{mol/L}$. The copper seed layer on top surface was only 80 nm, corresponding to sidewall seed thickness of ≈ 5 nm.

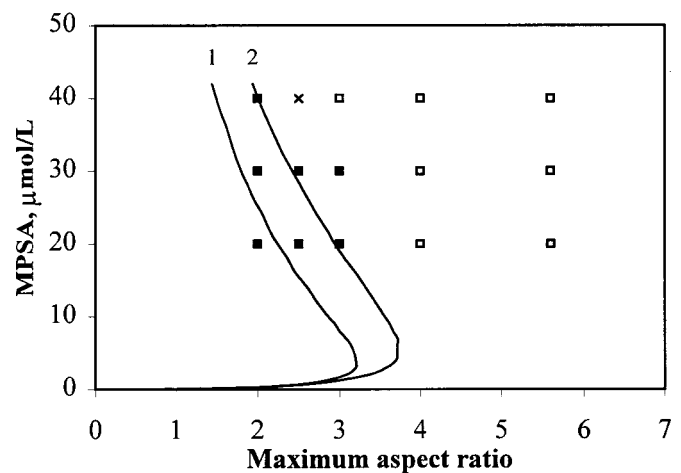
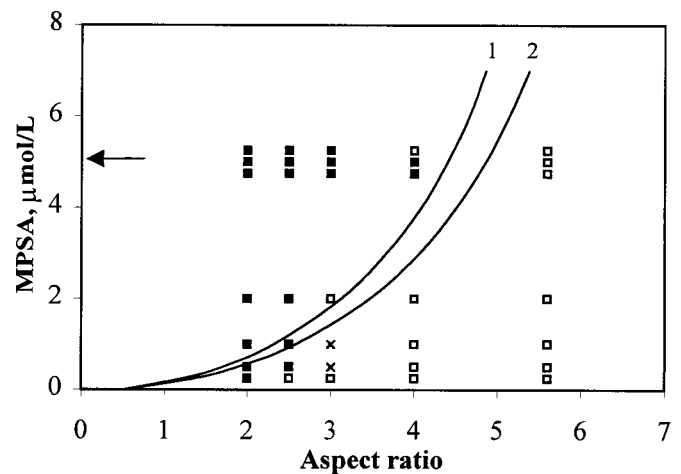


Figure 7. (a, top) Fill/fail boundaries predicted by the simple model for (1) -0.3 V and (2) -0.28 V are compared to experimental fill results at overpotentials of approximately -0.290 V as a function of the concentration of accelerator in the electrolyte. Filled squares indicate trenches that filled experimentally, while open squares indicate trenches that developed voids, and crosses indicate mixed results. (b, bottom) Similar results for overpotentials of approximately -0.150 V. Curve (1) -0.14 V and (2) -0.16 V.

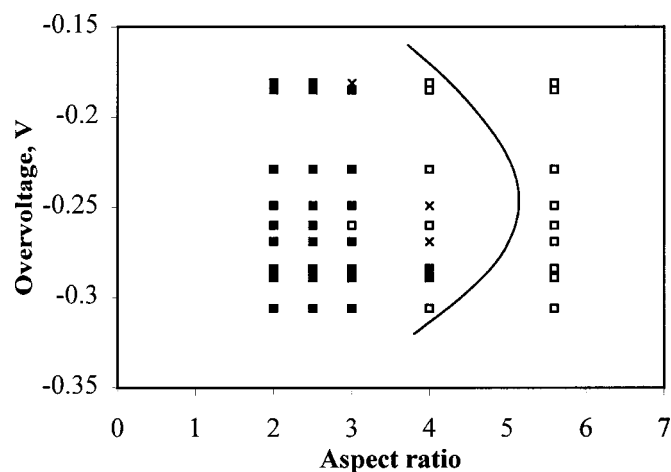


Figure 8. Fill/fail boundary predicted by the simple model is compared to experimental fill results for an accelerator concentration of $5 \mu\text{mol/L}$ as a function of the overpotential η during deposition. Filled squares indicate trenches that filled experimentally, while open squares indicate trenches that developed voids, and crosses indicate mixed results.

ited at overpotentials of between -0.284 and -0.306 V with fill/fail boundaries predicted by the simple model for representative overpotentials. Figure 7b compares experimental results for electrolytes with higher C_{MPSA} deposited at overpotentials of -0.149 to -0.158 V along with fill/fail boundaries predicted by the simple model for representative voltages. Figure 8 compares experimental results where the deposition voltage was varied between approximately -0.18 and -0.31 V for fixed additive concentration $C_{\text{MPSA}} = 5 \mu\text{mol/L}$ with the fill/fail boundary predicted by the simple model. Symbols are as in Fig. 7. The predictive ability, and thus usefulness, of the simple model is evident in both Fig. 7 and 8.

Conclusions

The simple model presented here has been shown to capture the behavior of trench filling by superconformal copper electrodeposition, predicting conditions for which fill can be expected. The simple model has been shown to give predictions that are consistent with a complete numerical solution, as implemented in the level-set code, upon which this simple model is based. The simple model yields the characteristic dependencies observed in the numerical solution, in spite of its geometric, diffusion, and accumulation simplifications. The computational simplicity of this model results in a code that can, in principle, evaluate over one thousand filling problems in the time that codes based on existing models of accumulation and growth evaluate one problem. This speed permits the thorough analysis of the superfill problem presented here.

The National Institute of Standards and Technology assisted in meeting the publication costs of this article.

References

1. P. C. Andricacos, *Electrochem. Soc. Interface*, **8**(1), 32 (1999).
2. P. C. Andricacos, C. Uzoh, J. O. Dukovic, J. Horkans, and H. Deligianni, *IBM J. Res. Dev.*, **42**, 567 (1998).
3. J. Reid and S. Mayer, in *Advanced Metallization Conference 1999*, p. 53, M. E. Gross, T. Gessner, N. Kobayashi, and Y. Yasuda, Editors, MRS, Warrendale, PA (2000).
4. T. Ritzdorf, D. Fulton, and L. Chen, in *Advanced Metallization Conference 1999*, p. 101, M. E. Gross, T. Gessner, N. Kobayashi, and Y. Yasuda, Editors, MRS, Warrendale, PA (2000).
5. E. Richard, I. Vervoort, S. H. Brongersma, H. Bender, G. Beyer, R. Palmans, S. Lagrange, and K. Maex, in *Advanced Metallization Conference 1999*, p. 149, M. E. Gross, T. Gessner, N. Kobayashi, and Y. Yasuda, Editors, MRS, Warrendale, PA (2000).
6. T. P. Moffat, J. E. Bonevich, W. H. Huber, A. Stanishevsky, D. R. Kelly, G. R. Stafford, and D. Josell, *J. Electrochem. Soc.*, **147**, 4524 (2000).
7. T. P. Moffat, D. Wheeler, W. H. Huber, and D. Josell, *Electrochem. Solid-State Lett.*, **4**, C26 (2001).
8. D. Josell, D. Wheeler, W. H. Huber, and T. P. Moffat, *Phys. Rev. Lett.*, **87**, 016102 (2001).
9. A. C. West, S. Mayer, and J. Reid, *Electrochem. Solid-State Lett.*, **4**, C50 (2001).
10. D. Wheeler, D. Josell, and T. P. Moffat, *J. Comput. Phys.*, Submitted.